Electronic Structure of the 16 Valence Electron Fragments $M(CO)_3(PR_3)_2$ (M = Mo, W; R = ^{i}Pr, Cy) in Their Complexes with H_2, THF, and Three π-Conjugated Dinucleating Ligands: Electrochemistry and Spectroscopy of Different Oxidation States

Wolfgang Bruns,[†] Wolfgang Kaim,*[,†] Eberhard Waldhör,[†] and Michael Krejcik[‡]

Institut für Anorganische Chemie der Universität, Pfaffenwaldring 55, D-70550 Stuttgart, Germany, and J. Heyrovsky Institute of Physical Chemistry and Electrochemistry, Czech Academy of Sciences, Dolejškova 3, CZ-18223 Prague, Czech Republic

Received July 19, 1994[⊗]

Mononuclear complexes *trans,mer*-$(PR_3)_2(CO)_3M(L)$ (M = Mo, W; R = ^{i}Pr, Cy; L = THF, η^2-H_2) and dinuclear complexes *trans,mer*-$[(PR_3)_2(CO)_3M]_2(\mu$-L) with the symmetrically bridging ligands μ-L = pyrazine (pz), 4,4′-bipyridine (bp) and 3,6-bis(4-pyridyl)-1,2,4,5-tetrazine (4,4′-bptz) were studied by cyclic voltammetry and by IR, UV/vis/near-IR, and EPR spectroscopy. Oxidation of the electron-rich and dissociatively labile (Mo > W) systems yields M(I) species, including stable ($K_c > 10^6$) mixed-valent d^5/d^6 cations $\{[(P^iPr_3)_2(CO)_3M]_2(pz)\}^+$. These mixed-valent complex ions exhibit complete delocalization on the vibrational time scale and show similar spectroscopic features as the structurally related Creutz−Taube ion $\{[(H_3N)_5Ru]_2(\mu$-pz)$\}^{5+}$. Reversible two-electron oxidation processes and thus no mixed-valent states were observed for the bp- and 4,4′-bptz-bridged ditungsten systems. Whereas the oxidation of $(PCy_3)_2(CO)_3W(\eta^2$-$H_2)$ is irreversible with the assumed loss of a proton, the solvates $(PR_3)_2(CO)_3M(THF)$ are reversibly oxidized and reduced, the latter process requiring rather negative potentials. In nonpolar solvents the neutral dinuclear complexes display very intense and strikingly narrow charge transfer bands in the near-infrared region, suggesting very little geometrical change between ground and MLCT excited states. One-electron reduction of the dinuclear complexes produces EPR-detectable radical anion complexes which show the loss of one PR_3 ligand per metal center, i.e. the preference for a 16 + δ rather than an 18 + δ valence electron configuration. The tungsten-centered oxidation of complexes $(PR_3)_2(CO)_3W(L)$ is facilitated in the order L = mpz^+, pz, H_2, 4,4′-bptz, bp, and THF, illustrating quantitatively the well-balanced σ donor and σ^* acceptor characteristics of the H_2 ligand. From the results of this study it appears that the $(PR_3)_2(CO)_3M$ fragments are suited to bind H_2 because of a very finely tuned combination of σ-acceptor and fairly strong but not excessive π-donor characteristics, in addition to the proper amount of steric shielding.

Introduction

Among the most unexpected[1] recent discoveries in chemistry has been the isolation and characterization of persistent complexes between the smallest neutral molecule, H_2, and low valent transition metal centers.[2−4] Although the side-on bonding of H_2 could be rationalized implicating $\sigma(H_2) \rightarrow d_{z^2}(M)$ and $d_{xz}(M) \rightarrow \sigma^*(H_2)$ components (Chart 1),[3,5,6] the special suitability of certain metal complexes, mostly 16 valence electron species with low-valent metal centers and at least some phosphane ligands,[2−4] has remained puzzling.

There have been extensive theoretical, structural, IR- and NMR-spectroscopic studies on complexes of the 16 valence electron "Kubas fragments" $(PR_3)_2(CO)_3M$, M = Mo, W,[2,5,7] especially of the η^2-H_2 complex.[2,3a,4] However, methods related to charge or electron transfer such as UV/vis absorption spectroscopy and (spectro)electrochemistry have not yet been systematically applied to these systems.

In the course of studies[8] aimed at elucidating the electronic structure of reversibly H_2-coordinating complex fragments we have recently reported[9] the spectroscopic, electrochemical and structural characterization of the unexpectedly stable compound $[(PCy_3)_2(CO)_3W(mpz)]^+$ (**I**) where mpz^+ is the excellent π acceptor ligand *N*-methylpyrazinium.[10,11] The very short

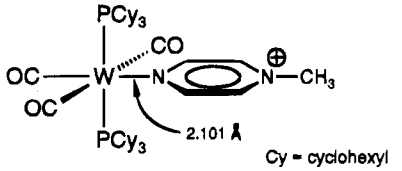

I

[†] Universität Stuttgart.
[‡] Czech Academy of Sciences.
[⊗] Abstract published in *Advance ACS Abstracts,* January 1, 1995.

(1) Basolo, F. *Coord. Chem. Rev.* **1993**, *125*, 13.
(2) (a) Kubas, G. J.; Ryan, R. R.; Swanson, B. S.; Vergamini, P. J.; Wasserman, H. J. *J. Am. Chem. Soc.* **1984**, *106*, 451. (b) Kubas, G. J.; Unkefer, C. J.; Swanson, B. I.; Fukushima, E. *J. Am. Chem. Soc.* **1986**, *108*, 7000. (c) Eckert, J.; Kubas, G. J.; Hall, J. H.; Hay, P. J.; Boyle, C. M. *J. Am. Chem. Soc.* **1990**, *112*, 2324. (d) Khalsa, G. R. K.; Kubas, G. J.; Unkefer, C. J.; Van der Sluys, L. S.; Kubat-Martin, K. A. *J. Am. Chem. Soc.* **1990**, *112*, 3855.
(3) (a) Kubas, G. J. *Acc. Chem. Res.* **1988**, *21*, 120. (b) Jessop, P. G.; Morris, R. H. *Coord. Chem. Rev.* **1992**, *121*, 155. (c) Morris, R. H. *Inorg. Chem.* **1992**, *31*, 1471. (d) Crabtree, R. H. *Angew. Chem.* **1993**, *105*, 828; *Angew. Chem., Int. Ed. Engl.* **1993**, *32*, 789. (e) Heinekey, P. M.; Oldham, W. J. *Chem. Rev.* **1993**, *93*, 913.
(4) Hay, P. J. *J. Am. Chem. Soc.* **1987**, *109*, 705.
(5) Saillard, J.-Y.; Hoffmann, R. *J. Am. Chem. Soc.* **1984**, *106*, 2006.
(6) (a) Burdett, J. K.; Phillips, J. R.; Pourian, M. R.; Poliakoff, M.; Turner, J. J.; Upmacis, R. *Inorg. Chem.* **1987**, *26*, 3054. (b) Burdett, J. K.; Pourian, M. R. *Inorg. Chem.* **1988**, *27*, 4445.
(7) (a) Wassermann, H. J.; Kubas, G. J.; Ryan, R. R. *J. Am. Chem. Soc.* **1986**, *108*, 2294. (b) Gonzalez, A. A.; Zhang, K.; Nolan, S. P.; Lopez de la Vega, R.; Mukerjee, S. L.; Hoff, C. D.; Kubas, G. J. *Organometallics* **1988**, *7*, 2429.
(8) (a) Bruns, W.; Kaim, W.; Ladwig, M.; Matheis, W.; Roth, T. In *Energieträger Wasserstoff*; VDI-Verlag: Düsseldorf, Germany, 1991; p 126. (b) Reinhardt, R.; Fees, J.; Klein, A.; Sieger, M.; Kaim, W. in *Wasserstoff als Energieträger*; VDI-Verlag: Düsseldorf; 1994, p 133.
(9) Bruns, W.; Hausen, H.-D.; Kaim, W.; Schulz, A. *J. Organomet. Chem.* **1993**, *444*, 121.
(10) Darby, W. L.; Vallarino, L. M. *Inorg. Chim. Acta* **1983**, *75*, 65.

0020-1669/95/1334-0663$09.00/0

Chart 1

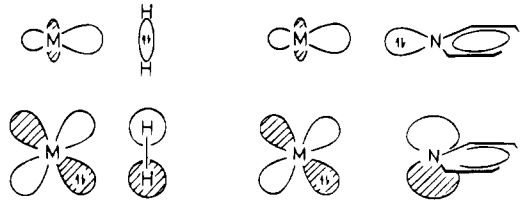

W−N(mpz$^+$) bond of only 2.101(10) Å suggested a strong π-type interaction (back donation) between the very weakly basic acceptor ligand and the electron-rich tungsten(0) center,[9] thus confirming qualitatively the pronounced capability of $(PR_3)_2(CO)_3W$ to donate dπ electrons and simultaneously accept electron density as put forward in the widely accepted model of side-on H_2 bonding (Chart 1).[3,5,6]

In this work we report electrochemical and EPR spectroelectrochemical data of the mononuclear complexes *trans,mer*-$(PR_3)_2(CO)_3M(L)$, L = THF, M = Mo (**1a**) or W (**2a,b**) and L = η^2-H_2, M = W, R = Cy (cyclohexyl) (**3b**). We also present a study of up to four available oxidation states of dinuclear compounds $[(PR_3)_2(CO)_3M(\mu\text{-}L)M(CO)_3(PR_3)_2]^n$, n = 1−,0,1+,2+; R = ^{i}Pr, Cy; μ-L = pyrazine (pz: **4a,b; 5a,b**),[12] 4,4′-bipyridine (bp: **6a**) and 3,6-bis(4-pyridyl)-1,2,4,5-tetrazine (4,4′-bptz: **7a**) (Chart 2). NMR, IR, UV/vis/near-IR and EPR spectroscopic data have been used to characterize the unusual electronic structures of neutral and neighboring paramagnetic states.

Experimental Section

Due to the lability of most complexes the synthetic, spectroscopic and electrochemical manipulations had to be carried out under an argon atmosphere in dried solvents.

Instrumentation and Procedures. ^{1}H-, ^{13}C-, and ^{31}P-NMR spectra were taken on Bruker spectrometers AM 200 or AC 250. EPR spectra were recorded in the X band on a Bruker System ESP 300 equipped with a Bruker ER035M gaussmeter and a HP 5350B microwave counter. Computer simulated spectra were obtained with the help of a self-written program.[13] Anionic complexes for EPR measurements were generated in THF or THF/[2.2.2] cryptand with distilled potassium metal in sealed glass tubes under high vacuum. Cationic complexes were obtained electrochemically (EPR spectroelectrochemistry) or by chemical oxidation with $AgPF_6$ or I_2. For infrared spectroscopy we used a Perkin-Elmer 684 spectrometer and a Philips PU 9800 FTIR instrument, spectroelectrochemistry was performed using an optically transparent thin-layer electrolytic "OTTLE" cell.[14] UV/vis/near-IR spectra were obtained using Shimadzu UV 160 and Bruins Instruments Omega 10 spectrometers (spectroelectrochemical measurements with the OTTLE cell[14]). Cyclic voltammetry experiments were performed in rigorously dried solvents containing 0.1 M Bu_4NClO_4 or 0.05 M Bu_4NBPh_4,[15a] using a three-electrode configuration (glassy carbon working electrode, Ag/AgCl reference, and Pt counter electrode), an EG&G PAR M273/M175 potentiostat and function generator; internal calibration was carried out with the ferrocene (Fc)/ferrocenium (Fc^+) pilot system.[15b,c] Elemental analyses were obtained using a Perkin-Elmer Analyzer 240. Carbide formation, insufficient combustion of the high molecular weight complexes, and the inevitable brief exposure to air during transfer resulted in sometimes unsatisfactory carbon values. The low nitrogen analysis of the bptz complex is typical for tetrazines with their rapid loss of N_2.

Chart 2

$(P^iPr_3)_2(CO)_3Mo(THF)$ **1a**

$(P^iPr_3)_2(CO)_3W(THF)$ **2a**

$(PCy_3)_2(CO)_3W(THF)$ **2b**

$(PCy_3)_2(CO)_3W(H_2)$ **3b**

$[(P^iPr_3)_2(CO)_3Mo]_2(\mu\text{-pz})$ **4a**

$[(PCy_3)_2(CO)_3Mo]_2(\mu\text{-pz})$ **4b**

$[(P^iPr_3)_2(CO)_3W]_2(\mu\text{-pz})$ **5a**

$[(PCy_3)_2(CO)_3W]_2(\mu\text{-pz})$ **5b**

$[(P^iPr_3)_2(CO)_3W]_2(\mu\text{-bp})$ **6a**

$[(P^iPr_3)_2(CO)_3W]_2(\mu\text{-4,4'-bptz})$ **7a**

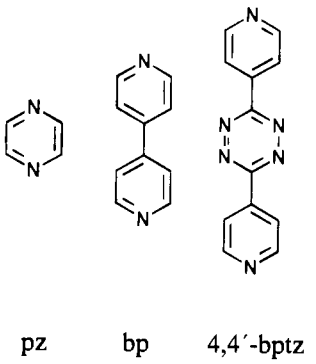

Syntheses. The ligand 3,6-bis(4-pyridyl)-1,2,4,5-tetrazine (4,4′-bptz),[16] the metal species $M(CO)_3(PR_3)_2$, and their THF (**1, 2**) and dihydrogen complexes (**3**)[2,7] were obtained following literature procedures, involving dinitrogen complex intermediates for the Mo derivatives.[2b,7]

***trans,mer*-(μ-Pyrazine)bis(bis(triisopropylphosphane)tricarbonylmolybdenum(0)), $[(P^iPr_3)_2(CO)_3Mo]_2(\mu\text{-pz})$, 4a.** Addition of 0.571 g (1.14 mmol) of $(P^iPr_3)_2(CO)_3Mo$ to 0.046 g (0.57 mmol) of pyrazine in 9 mL of toluene yielded a dark-blue solution which changed to dark-green after stirring for 2 h. The precipitated solid was filtered off, washed with toluene (about 1 mL), and dried under vacuum to yield 0.42 g (68%) of the dark-green microcrystalline product. ^{1}H-NMR (C_6D_6): δ 7.82 (s, 4H), 2.20 (m, 12H), 1.20 (dd, 72H); $^3J_{HH}$ = 7.1 Hz, $^3J_{HP}$ = 13.1 Hz. ^{31}P-NMR (C_6D_6): δ 54.9. Anal. Calcd for $C_{46}H_{88}Mo_2N_2O_6P_4$ (1081.0): C, 51.11; H, 8.21; N, 2.59. Found: C, 50.91; H, 8.38; N, 2.52.

***trans,mer*-(μ-Pyrazine)bis(bis(tricyclohexylphosphane)tricarbonylmolybdenum(0)), $[(PCy_3)_2(CO)_3Mo]_2(\mu\text{-pz})$, 4b.** An amount of 157 mg (0.21 mmol) of $(PCy_3)_2(CO)_3Mo$ and 7.2 mg (0.09 mmol) of pyrazine were added in 2 mL of toluene and stirred for 6 h. The precipitated blue solid (80 mg, 57%) filtered off the dark-blue solution is virtually insoluble in noncoordinating solvents. Anal. Calcd for $C_{82}H_{136}Mo_2N_2O_6P_4$ (1561.8): C, 63.06; H, 8.78; N, 1.79. Found: C, 62.29; H, 8.78; N, 1.05.

***trans,mer*-(μ-Pyrazine)bis(bis(triisopropylphosphane)tricarbonyltungsten(0)), $[(P^iPr_3)_2(CO)_3W]_2(\mu\text{-pz})$, 5a.** Addition of 1.14 g (1.94 mmol) of $(P^iPr_3)_2(CO)_3W$ to 0.077 g (0.97 mmol) of pyrazine in 15 mL of toluene yielded a blue-green solution which changed to dark-green within minutes. After this was stirred for 6 h, the precipitated solid was filtered off, washed with 1−2 mL of toluene and dried under vacuum to yield 0.90 g (74%) of the dark-green microcrystalline product. ^{1}H-NMR (C_6D_6): δ 7.81 (s, 4H), 2.25 (m, 12H), 1.21 (dd, 72H); $^3J_{HH}$ = 7.2 Hz, $^3J_{HP}$ = 12.4 Hz. ^{13}C-NMR (C_6D_6): δ 212.2 (weak, CO), 147.8 (s, pz), 27.8 (t, CH), 19.9 (s, CH_3); $^1J_{CP}$ = $^3J_{CP}$ = 8.2 Hz. ^{31}P-NMR (C_6D_6): δ 34.9; $^1J_{WP}$ = 270 Hz. Anal. Calcd for $C_{46}H_{88}N_2O_6P_4W_2$ (1256.8): C, 43.96; H, 7.06; N, 2.23. Found: C, 43.89; H, 7.22; N, 2.19.

***trans,mer*-(μ-Pyrazine)bis(bis(triisopropylphosphane)-tricarbonyltungsten(0.5)) Tetraphenylborate, $\{[(P^iPr_3)_2(CO)_3W]_2(\mu\text{-pz})\}(BPh_4)$, $(5a^+)(BPh_4)$.** A solution of 1.57 g (1.25 mmol) of **5a** and 0.85 g (2.50 mmol) of $NaBPh_4$ in 30 mL of dichloromethane was

(11) (a) Creutz, C.; Chou, M. H. *Inorg. Chem.* **1987**, *26*, 2995. (b) Wishart, J. F.; Bino, A.; Taube, H. *Inorg. Chem.* **1986**, *25*, 3318. (c) Poppe, J.; Kaim, W.; Ben Altabef, A.; Katz, N. E. *J. Chem. Soc., Perkin Trans. 2* **1993**, 2105.

(12) (a) Bruns, W.; Kaim, W. *J. Organomet. Chem.* **1990**, *390*, C45. (b) Bruns, W.; Kaim, W. in *Mixed Valency Systems − Applications in Chemistry, Physics and Biology* (Prassides, K., ed.); Kluwer Academic Publishers: Dordrecht; 1991, p 365. (c) Kaim, W.; Bruns, W.; Poppe, J.; Kasack, V. *J. Mol. Struct.* **1993**, *292*, 221. (d) Bruns, W.; Kaim, W.; Waldhoer, E.; Krejcik, M. *J. Chem. Soc., Chem. Commun.* **1993**, 1868.

(13) Bruns, W. Ph.D. Thesis, Universität Stuttgart, 1993.

(14) Krejcik, M.; Danek, M.; Hartl, F. *J. Electroanal. Chem.* **1991**, *317*, 179.

(15) (a) Abbott, A. *Chem. Soc. Rev.* **1993**, 435. (b) Gritzner, G.; Kuta, J. *Pure Appl. Chem.* **1984**, *56*, 461. (c) Bond, A. M.; McLennan, E. A.; Stojanovic, R. S.; Thomas, F. G. *Anal. Chem.* **1987**, *59*, 2853.

(16) Kaim, W.; Kohlmann, S. *Inorg. Chem.* **1990**, *29*, 1898. The lowest unoccupied orbitals involved are a_u (tetrazine-centered) and b_{1u} (delocalized, previously referred to as a_u').

Table 1. Electrochemical Data of Ligands and Complexes[a]

compd	E_{ox2}	E_{ox1}	E_{red1}	E_{red2}	electrolyte
1a		−0.60 (90)	−2.55 (85)	−3.16 (pc)	THF/0.05 M Bu_4NBPh_4
2a		−0.69 (65)	−2.45 (80)		THF/0.05 M Bu_4NBPh_4
2b		−0.69 (85)	−2.50 (80)	−3.13 (pc)	THF/0.05 M Bu_4NBPh_4
3b		−0.40 (pa)[b]			THF/0.05 M Bu_4NBPh_4
pz			−2.60 (90)		THF/0.1 M Bu_4NClO_4
4a[c]	+0.01 (120)	−0.37 (100)	−1.95 (110)		THF/0.1 M Bu_4NClO_4
5a	−0.01 (60)	−0.51 (65)	−1.96 (65)		THF/0.1 M Bu_4NClO_4
5a	−0.01 (75)	−0.66 (70)	−2.00 (70)		CH_2Cl_2/0.1 M Bu_4NClO_4
5a	−0.01 (80)	−0.71 (75)	−2.05 (80)		THF/0.05 M Bu_4NBPh_4
bp			−2.47 (100)	−2.90 (160)	THF/0.05 M Bu_4NBPh_4
6a	−0.48 (80)[d]		−1.94 (65)	−2.75 (100)[c]	THF/0.05 M Bu_4NBPh_4
4,4′-bptz			−1.24 (70)	−2.49 (pc)	THF/0.05 M Bu_4NBPh_4
7a	−0.43 (90)[d]		−1.22 (80)	−2.11 (80)	THF/0.05 M Bu_4NBPh_4

[a] Potentials in V vs Fc/Fc^+ (internal calibration), peak potential differences in mV (in parentheses). From cyclic voltammetry at 100 mV/s unless noted otherwise. pa: anodic peak potential, pc: cathodic peak potential for irreversible process. [b] At 200 mV, external calibration against Fc/Fc^+, cathodic signal at $E_{pc} = -0.76$ V. [c] At 500 mV/s. [d] Two-electron wave.

treated with small portions of iodine until the IR and UV/vis spectra indicated the disappearance of the neutral complex. Sodium iodide and excess $NaBPh_4$ were filtered off and the blue-green filtrate was concentrated to about 4 mL. On addition of 10 mL of *n*-hexane, a blue-green microcrystalline solid precipitated in 1.67 g (85%) yield. Anal. Calcd for $C_{70}H_{108}BN_2O_6P_4W_2$ (1576.0): C, 53.35; H, 6.91; N, 1.78. Found: C, 51.93; H, 6.52; N, 1.59.

***trans,mer*-(μ-Pyrazine)bis(bis(tricyclohexylphosphane)tricarbonyltungsten(0)), $[(PCy_3)_2(CO)_3W]_2(\mu\text{-pz})$, 5b.** A sample of 525 mg (0.63 mmol) of $(PCy_3)_2(CO)_3W$ and 25 mg (0.31 mmol) of pyrazine were added in 6 mL of toluene and stirred for 6 h. The precipitated greenish solid (389 mg, 71%) filtered off is virtually insoluble in noncoordinating solvents. Anal. Calcd for $C_{82}H_{136}N_2O_6P_4W_2$ (1737.7): C, 58.68; H, 7.89; N, 1.61. Found: C, 57.22; H, 7.97; N, 1.27.

***trans,mer*-(μ-4,4′-Bipyridine)bis(bis(triisopropylphosphane)tricarbonyltungsten(0)), $[(P^iPr_3)_2(CO)_3W]_2(\mu\text{-bp})$, 6a.** Addition of 870 mg (1.48 mmol) of $(P^iPr_3)_2(CO)_3W$ and 115 mg (0.47 mmol) of 4,4′-bipyridine in 17 mL of toluene yielded a dark blue solution from which a blue-black precipitate was filtered off after stirring for 4 h. Washing with 1−2 mL of toluene and drying under vacuum yielded 871 mg (88%) of the very sensitive product. Anal. Calcd for $C_{52}H_{92}N_2O_6P_4W_2$ (1332.9): C, 46.86; H, 6.96; N, 2.10. Found: C, 48.06; H, 6.93; N, 1.97.

***trans,mer*-(μ-3,6-Bis(4-pyridyl)-1,2,4,5-tetrazine)bis(bis(triisopropylphosphane)tricarbonyltungsten(0)), $[(P^iPr_3)_2(CO)_3W]_2(\mu\text{-}4,4'\text{-bptz})$, 7a.** A suspension of 590 mg (1.00 mmol) of $(P^iPr_3)_2(CO)_3W$ and 100 mg (0.42 mmol) of 4,4′-bptz in 8 mL of toluene was stirred for six hours. Filtration and drying under vacuum yielded 127 mg (23%) of the sensitive blue-black product. Anal. Calcd for $C_{54}H_{92}N_6O_6P_4W_2$ (1412.6): C, 45.90; H, 6.56; N, 5.95. Found: C, 45.27; H, 6.68; N, 5.28.

Results

THF and η^2-H_2 Complexes. Compounds $(PR_3)_2(CO)_3M$ which form cyclic structures with agostic C−H- - -M interactions in the solid state[7a] were studied electrochemically in dry THF solutions where they form purple solvates with $\lambda_{max} \approx$ 550 nm. The use of other coordinating (acetonitrile, DMF) or chlorinated solvents (CH_2Cl_2, ClH_2CCH_2Cl) or of conventional electrolytes such as Bu_4NPF_6 or Bu_4NClO_4 did not give satisfactory cyclovoltammetric results, however, Bu_4NBPh_4 in THF proved to be a suitable system (Figure 1, Table 1). Reversible oxidation processes were observed at a moderate potential, leading to labile but EPR detectable M(I) species (d^5 configuration); *g* factor components are listed in Table 2. Quasi-reversible reduction processes to anionic M(−I) species (d^7) occur at rather negative potentials (Figure 1, Table 1).

Under 1 atm of pressure of H_2 in THF/0.05 M Bu_4NBPh_4 the yellow complex $(PCy_3)_2(CO)_3W(\eta^2\text{-}H_2)$ is formed[2] which could be oxidized, albeit irreversibly at a positive potential

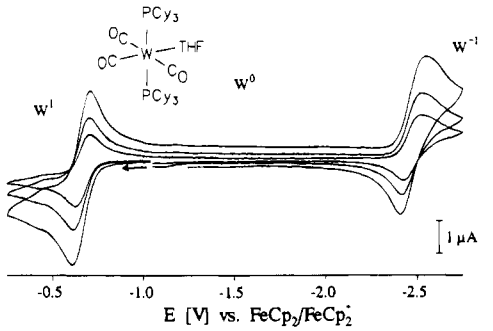

Figure 1. Cyclic voltammograms of $(PCy_3)_2(CO)_3W(THF)$ (**2b**) in THF/0.05 M Bu_4NBPh_4 at 100, 200, and 500 mV/s scan rate (in the order of increasing currents).

Table 2. EPR Data of Cationic Complexes

complex	g_1	g_2	g_3	g_{iso}	*T* (K)	medium
$\mathbf{1a}^+$	2.097	2.065	1.994	2.052	110	THF/0.05 MBu_4NBPh_4[a]
$\mathbf{2a}^+$	2.250	2.147	1.973	2.126	110	THF/0.05 M Bu_4NBPh_4[a]
$\mathbf{4a}^+$	2.0655	2.0655	1.9755	2.036	110	CH_2Cl_2[b]
$\mathbf{4a}^+$				2.0438[c]	298	CH_2Cl_2[b]
$\mathbf{5a}^+$				2.102[d]	298	CH_2Cl_2, PF_6^- salt[e]
$\mathbf{5a}^+$	2.197	2.158	1.931	2.099	110	CH_2Cl_2/0.1 M Bu_4NClO_4[a]

[a] Electrolytic generation. [b] From oxidation with $FcPF_6$. [c] Peak-to-peak line width $\Delta H_{pp} = 1.4$ mT; $a(^{95,97}Mo) = 1.52$ mT, the corresponding mononuclear Mo(I) complex has $a(^{95,97}Mo) = 2.6$ mT.[12d] [d] $\Delta H_{pp} = 5.5$ mT. [e] From oxidation of **5a** with $AgPF_6$.

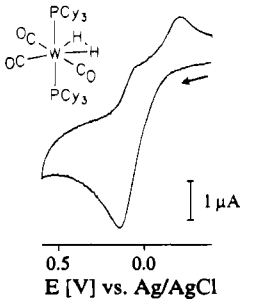

Figure 2. Cyclic voltammogram of $(PCy_3)_2(CO)_3W(H_2)$ (**3b**) in THF/0.05 M Bu_4NBPh_4 at 200 mV/s scan rate.

relative to the THF solvate. A small rereduction peak was observed at more negative values (Figure 2). Due to the lability of H_2 complexes[2] an external calibration with the ferrocene/ferrocenium pair had to be applied; all other tested dihydrogen complexes $(PR_3)_2(CO)_3M(H_2)$ did not give satisfactory cyclovoltammetric responses.

Dinuclear Complexes. All PCy_3-containing dinuclear complexes exhibit very low solubility; most of the relevant results

Table 3. Carbonyl Vibrational Frequencies ν_{CO} (cm^{-1}) of Complexes in Various Oxidation States

complex	$b_{1u}(1)$	b_{2u}	$b_{1u}(2)$
4a[a]	1932 (m)	1801 (s)	1829 (vs)
4a$^+$ [a]	1962 (s)	1898 (s)	1871 (vs)
4b[b]	1928 (s)	1804 (vs)	1823 (s)
5a[a]	1922 (s)	1798 (s)	1820 (vs)
5a$^+$ [a]	1964 (vs)	1894 (s)	1866 (vs)
5a^{2+} [a,c]	2026 (m)	2010 (s)	1926 (s)
5b[b]	1920 (s)	1800 (vs)	1814 (vs)
6a[d]	1922 (s)	1804 (vs)	1785 (vs)
7a[d]	1922 (s)	1804 (vs)	1785 (s)

[a] From spectroelectrochemistry in CH_2Cl_2/0.1 M Bu_4NPF_6. [b] In Nujol. [c] Rapidly decomposing. [d] In CH_2Cl_2.

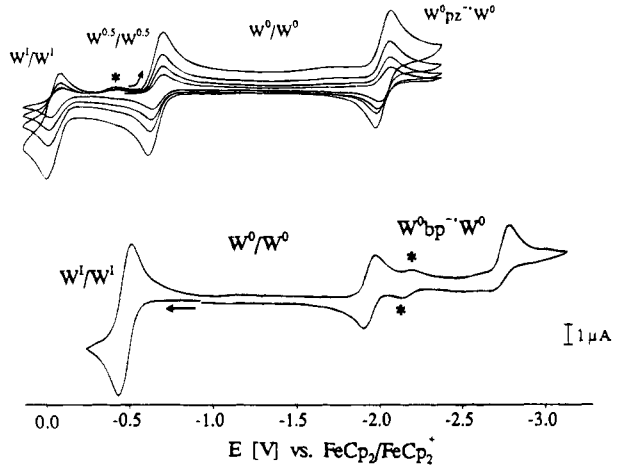

Figure 3. Top: Cyclic voltammograms of $[(P^iPr_3)_2(CO)_3W]_2(\mu\text{-pz})$ (**5a**) in CH_2Cl_2/0.1 M Bu_4NClO_4 at 50, 100, 200 and 500 mV/s scan rate; (*) decomposition product occurring after second oxidation. Bottom: Cyclic voltammogram of $[(P^iPr_3)_2(CO)_3W]_2(\mu\text{-bp})$ (**6a**) in THF/0.05 M Bu_4NBPh_4 at 100 mV/s scan rate; (*) reduction of mononuclear compound formed by dissociation.

reported here were thus obtained with the P^iPr_3-containing compounds. In general, the molybdenum complexes are less stable than the tungsten compounds; therefore, only a few Mo analogues of the W species could be synthesized and studied. The dinuclear complexes were characterized by chemical and instrumental analysis (^1H-, ^{13}C-, ^{31}P-NMR and IR; see Experimental Section and Table 3). The conformation is assumed to be as determined for *trans,mer*-$[(PCy_3)_2(CO)_3W(mpz)]^+$ (**I**), i.e. with the bulky phosphanes in axial position to the plane containing the $M(CO)_3$ fragment and the heterocycle.[9]

As previously described[12] the dinuclear pyrazine complexes $[(P^iPr_3)_2(CO)_3M]_2(\mu\text{-pz})$ exhibit two reversible and well-separated one-electron oxidation steps and one apparently reversible reduction wave (Figure 3, Table 1). As the first oxidation potentials are rather low, one mixed-valent species could be isolated via controlled oxidation with iodine as a fairly stable tetraphenylborate salt, (**5a**$^+$)(BPh_4^-). The dinuclear pyrazine complexes were studied by IR (Figure 4), UV/vis/near-IR (Figures 5–7), and EPR spectroscopy (Figures 8 and 9) or spectroelectrochemistry (Tables 1–5); due to their sensitivity, the dicationic and monoanionic states could be investigated only in a few instances (see Figures 4 and 9).

The use of bridging 4,4′-bipyridine or 3,6-bis(4-pyridyl)-1,2,4,5-tetrazine[16] instead of pyrazine for the $(P^iPr_3)_2(CO)_3W$ fragment results in a much diminished stability of the neutral complexes towards dissociation into mononuclear forms and in a coincidence of both one-electron oxidation waves; a mixed-valent form is thus nonexistent (Figure 3). However, apparently

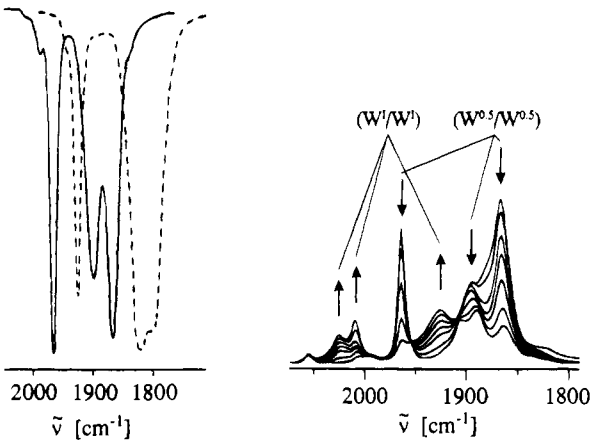

Figure 4. Left: Carbonyl vibrational spectra of $[(P^iPr_3)_2(CO)_3W]_2(\mu\text{-pz})$ (**5a**) (- - -) and **5a**$^+$(BPh_4^-) (—) in CH_2Cl_2. Right: FTIR spectroelectrochemistry of the redox pair **5a**$^+$/**5a**$^{2+}$ in CH_2Cl_2/0.1 M Bu_4NPF_6 (weak electrolyte signals at 2055 and 1890 cm^{-1}).

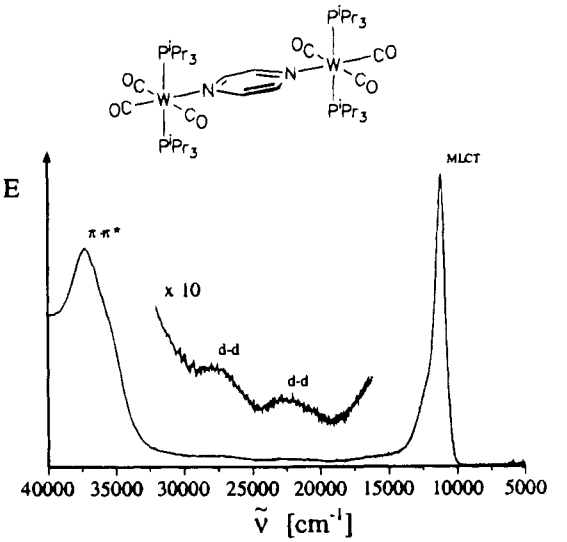

Figure 5. Absorption spectrum (wave number scale) of $[(P^iPr_3)_2(CO)_3W]_2(\mu\text{-pz})$ (**5a**) in CH_2Cl_2.

reversible one-electron reduction processes were observed for both complexes **6a** and **7a** with the longer π-conjugated ligands (Table 1).

Cationic (Mo, W) and dicationic forms (W) of the pyrazine-bridged complexes were sufficiently stable to be studied by infrared spectroelectrochemistry. A simple comparison of the isolated species **5a**, (**5a**$^+$)(BPh_4^-) (Figures 4 and 7), and the spectroelectrochemically generated dication **5a**$^{2+}$ (Figure 4) shows the expected[17] high-energy shift of the carbonyl stretching bands on metal oxidation (Table 3); however, there is *only one* set of carbonyl bands corresponding to a meridional substitution pattern in each oxidation state. Both transitions o/+[12c] and +/2+ (Figure 4) are characterized by isosbestic points in the vibrational spectra.

All neutral dinuclear complexes **4a**–**7a** with the π-accepting ligands L exhibit an intense and narrow charge transfer (CT) band with a high-energy shoulder in the near-infrared region, in addition to a number of much weaker bands in the visible (Figure 5). A detailed study of the CT band of complex **5a** showed a distinct solvent dependence of the bandwidth and of

(17) (a) Atwood, C. G.; Geiger, W. E. *J. Am. Chem. Soc.* **1993**, *115*, 5310. (b) Zhang, Y.; Gosser, D. K.; Rieger, P. H.; Sweigart, D. A. *J. Am. Chem. Soc.* **1991**, *113*, 4062.

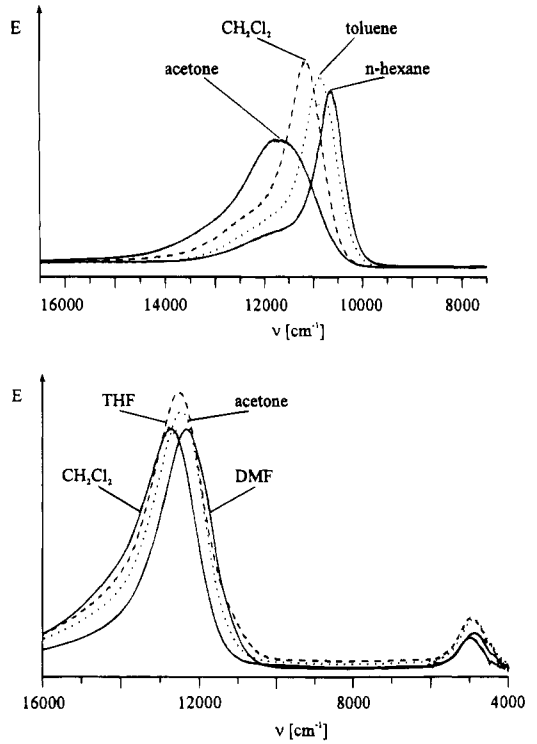

Figure 6. Solvent effects on MLCT and MMCT bandwidths and band maxima: top, compound [(P^{i}Pr$_3$)$_2$(CO)$_3$W]$_2$(μ-pz) (**5a**); bottom, oxidized form **5a**$^+$; different absorbance for each spectrum.

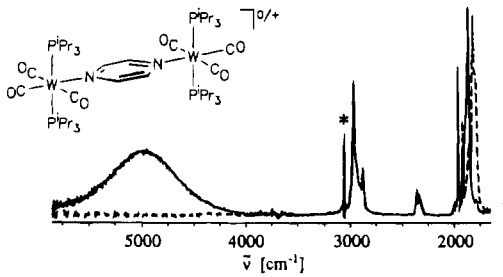

Figure 7. IR/near-IR spectra of [(P^{i}Pr$_3$)$_2$(CO)$_3$W]$_2$(μ-pz) **5a** (- - -) and **5a**$^+$ (—) from spectroelectrochemistry in CH_2Cl_2/0.1 M Bu_4NPF_6; (*) electrolyte signal.

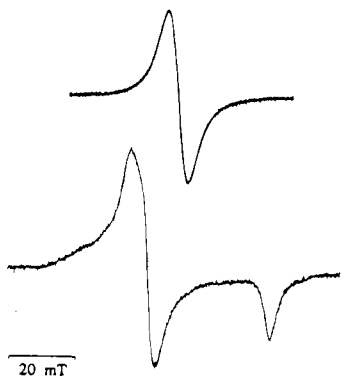

Figure 8. EPR spectra of [(P^{i}Pr$_3$)$_2$(CO)$_3$W]$_2$(μ-pz)$^+$ (**5a**$^+$) at room temperature and at 110 K in fluid (top) and frozen CH_2Cl_2 solution (bottom).

the absorption maximum (negative solvatochromism;[18] Figure 6 and Table 4). On one-electron oxidation of the pyrazine-bridged complexes there is a slight hypsochromic shift and broadening of the CT band which now exhibits a very small

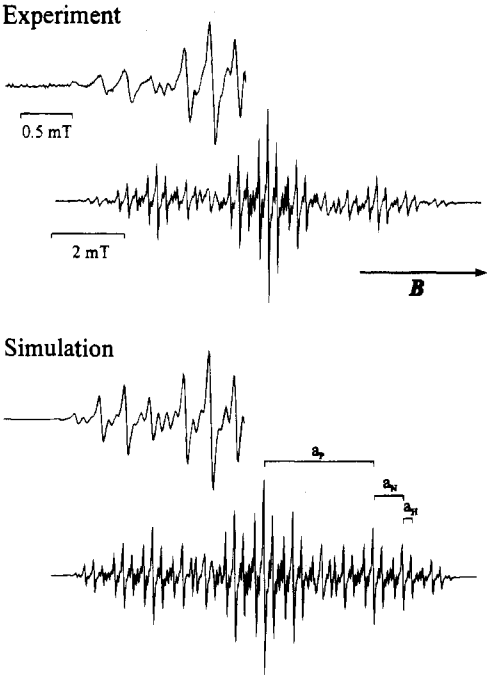

Figure 9. Top: EPR spectrum of the reduction product of [(P^{i}Pr$_3$)$_2$(CO)$_3$W]$_2$(μ-pz) (**5a**) after treatment with K in THF/1 mM [2.2.2] cryptand. Bottom: Computer-simulated spectra with the data from Table 5 and 0.041 mT line width.

positive[18] solvatochromism (Table 4). However, the essential new feature is the emergence of a symmetrical and fairly intense band in the near infrared region. This band is barely solvatochromic (Figure 6), and it occurs at longer wavelength for the Mo complex **4a**$^+$ than for the tungsten analogue **5a**$^+$. Its origin from an electronic transition is obvious from the comparison in Figure 7 which demonstrates the proximity of vibrational and electronic transitions.

EPR results were obtained for both paramagnetic forms of the dinuclear complexes. The monocationic states of the pyrazine-bridged complexes show rather broad solution spectra (Figure 8) with no observable ^{31}P hyperfine splitting; due to the smaller line width of the molybdenum system with its much lower moment of inertia, $\Theta = \sum m_i r_i^2$, and more rapid rotation in solution, a ^{95,97}Mo coupling could be detected.[12d] In frozen solution, the monocations exhibit essentially axial EPR spectra with slight rhombic perturbation and a relatively small g anisotropy (Figure 8). Metal isotope or ^{31}P hyperfine components could not be established.

Highly resolved solution EPR spectra of the anionic forms of the complexes were obtained by reaction of the neutral complexes with potassium in THF containing small amounts of [2.2.2] cryptand for better cation complexation. Computer simulations of the hyperfine structures involving ^{1}H, ^{14}N, ^{31}P and metal isotope coupling parameters were only successful (Figure 9) when an unusually large coupling from a *single* ^{31}P nucleus for each metal center was included in what are otherwise clearly symmetrical radical complexes.[19,20]

Discussion

THF Complexes. The high reactivity of the "Kubas-type" complexes (PR$_3$)$_2$(CO)$_3$M(L), including L = H_2, precluded the use of conventional electrolytes because of reactions of the 16 valence electron fragments with perchlorate or hexafluorophos-

(18) (a) Manuta, D. M.; Lees, A. J. *Inorg. Chem.* **1983**, *22*, 3825. (b) Kaim, W.; Kohlmann, S.; Ernst, S.; Olbrich-Deussner, B.; Bessenbacher, C.; Schulz, A. *J. Organomet. Chem.* **1987**, *321*, 215.

(19) Kaim, W. *Coord. Chem. Rev.* **1987**, *76*, 187.

(20) (a) Kaim, W. *Inorg. Chim. Acta* **1981**, *53*, L151. (b) Kaim, W. *J. Organomet. Chem.* **1984**, *262*, 171.

Table 4. Absorption Data of Dinuclear Complexes in Different Solvents and Oxidation States[a]

		MLCT		MMCT		LF
complex	solvent	ν	$\Delta\nu_{1/2}$	ν	$\Delta\nu_{1/2}$	ν
4a	CH_2Cl_2	11530	1280			*b*
	toluene	11770	1300			*b*
	THF	12220	1940			*b*
4a$^+$	CH_2Cl_2	12100	1940	4650[c]	700	*b*
5a	*n*-hexane	10580	690			
	cyclohexane	10630	700			
	toluene	10850[d,e]	850			15500 sh, 22700, 27400[f]
	benzene	10930	850			
	CH_2Cl_2	11040[e]	940			15500 sh, 22600, 27600
	THF	11270	1490[g]			
	CH_3CN	11480	1200[g]			
	acetone	11680	1740			
	DMF	11950	1860			
5a$^+$	CH_2Cl_2	12720[h]	1760	4990[i]	730	18000 sh, 26900, 31900 sh[f]
	THF	12530	1680	4940	750	
	CH_3CN	12530	1640	4950	750	18000 sh, 26700, 32000 sh
	acetone	12470	1630	4930	760	
	DMF	12180	1880	4900	780	
5b	toluene	9880	1700			
	CH_2Cl_2	9950	1300			
	CH_3CN	11000	*j*			
6a	THF	12780	5000[g]			*b*
7a	toluene	8900	*b*			*b*

[a] Wave numbers ν (cm^{-1}) at the absorption maxima, band widths $\Delta\nu_{1/2}$ at half height. [b] Not available with certainty due to the lability of the complex. [c] Molar extinction coefficient $\epsilon = 7000\ M^{-1}\ cm^{-1}$. [d] $\epsilon = 77000\ M^{-1}\ cm^{-1}$. [e] Shoulder at 12000 cm^{-1}. [f] $\epsilon \approx 10^3\ M^{-1}\ cm^{-1}$. [g] Unsymmetrical band. [h] $\epsilon = 29000\ M^{-1}\ cm^{-1}$. [i] $\epsilon = 4600\ M^{-1}\ cm^{-1}$. [j] Not determined due to low *S/N* ratio (low solubility).

Table 5. EPR Data of Anionic Ligands and Complexes[a]

radical	$a(^{14}N)$	$a(^1H)$	$a(^{31}P)$	$a(M)^b$	*g*	ref
$pz^{-\bullet}$	0.718	0.264			2.0035	20a,b
$(pz^{-\bullet})[Mo(CO)_5]_2$	0.818	0.254		0.150	2.0042	20a,b
$(pz^{-\bullet})[Mo(CO)_4(P^nBu_3)]_2$	0.808	0.247	1.150	0.152	2.0042	20b
$(pz^{-\bullet})[Mo(CO)_3(P^iPr_3)]_2$[c]	0.801	0.246	2.583	0.172	2.0043	this work
$(pz^{-\bullet})[W(CO)_5]_2$	0.823	0.254		0.286	2.0061	20a,b
$(pz^{-\bullet})[W(CO)_4(P^nBu_3)]_2$	0.815	0.243	1.307	0.295	2.0057	20b
$(pz^{-\bullet})[W(CO)_4(P(OMe)_3)]_2$	0.808	0.240	1.075	0.283	2.0058	20b
$(pz^{-\bullet})[W(CO)_4(P^iPr_3)]_2$	0.810	0.243	1.228	0.294	2.0057	20b
$(pz^{-\bullet})[W(CO)_3(P^iPr_3)]_2$[c]	0.798	0.240	2.995	0.318	2.0059	this work
$bp^{-\bullet}$	0.362	0.440/ 0.237[d]			2.0032	20a,b
$(bp^{-\bullet})[W(CO)_5]_2$	0.433	0.080/ 0.192[d]		0.163	2.0050	20a,b
$(bp^{-\bullet})[W(CO)_4(P(OMe)_3)]_2$	0.442	0.072/ 0.199[d]	0.570	n.d.	2.0047	20b
$(bp^{-\bullet})[W(CO)_3(P^iPr_3)]_2$[c]	0.432	0.059/ 0.199[d]	1.502	0.22	2.0049	this work
4,4′-$bptz^{-\bullet}$	0.493[e]				2.0041	16
(4,4′-$bptz^{-\bullet}$)$[W(CO)_5]_2$	0.488[e]				2.0039	16
(4,4′-$bptz^{-\bullet}$)$[W(CO)_3(P^iPr_3)_n]_2$[c]	0.500[e]				2.0040	this work

[a] Isotropic coupling constants *a* in mT; radical anion generation with K in THF or THF/[2.2.2] cryptand. [b] $^{95,97}Mo$ ($I = 5/2$, 25.4% combined natural abundance) or ^{183}W ($I = 1/2$; 14.3%). [c] From corresponding bis(bis(phosphane)metal) complexes **4a**, **5a**, **6a**, or **7a**. [d] $a(H^2)/a(H^3)$. [e] Four equivalent tetrazine N, no other hyperfine coupling observed.

phate.[21] A 0.05 M tetrabutylammonium tetraphenylborate[15a] solution in dry THF turned out to be a superior electrolyte system; chlorinated hydrocarbons reacted irreversibly with the compounds.

Solutions of the complexes $(PR_3)_2(CO)_3M$ in THF exhibit reversible oxidation and reduction behavior, the latter with slightly diminished reversibility at rather negative potentials. Considering the ligand set, it is not surprising that the electron-rich M(0) species, most likely the solvates $(PR_3)_2(CO)_3M(THF)$, are oxidized rather easily. The resulting M(I) cations with their d^5 configuration exhibit a typical rhombic EPR appearance in frozen THF solution (Table 2), similar to that reported for the related M(I) carbonyl systems *trans*-$W(CO)_4(olefin)_2$ ($g_1 \approx 2.26$, $g_2 \approx 2.15$, $g_3 \approx 1.88$).[22]

Remarkably, the THF solvates can also be one-electron reduced if only at rather negative potentials. The resulting M(−I) systems with low-spin d^7 configuration are assumed to be pentacoordinate via loss of THF, in agreement with the established structure for neutral *trans*-$(PCy_3)_2(CO)_3Re$[23a,b] and other low-spin d^7 systems such as $[Co(CN)_5]^{3-}$ or $NiBr_3$-

(21) Cf. the coordination of BF_4^- to tungsten in $(PCy_3)_2(CO)_3HW(BF_4)$: Van Der Sluys, L. S.; Kubat-Martin, K. A.; Kubas, G. J.; Caulton, K. G. *Inorg. Chem.* **1991**, *30*, 306.

(22) Wilgocki, M.; Szymanska-Buzar, T.; Jaroszewski, M.; Ziolkowski, J. J. in *Molecular Electrochemistry of Inorganic, Bioinorganic and Organometallic Compounds* (Pombeiro, A. J. L.; McCleverty, J. A., eds.); Kluwer Academic Publishers: Dordrecht; 1993, p 573.

(23) (a) Walker, H. W.; Rattinger, G. B.; Belford, R. L.; Brown, T. L. *Organometallics* **1983**, *2*, 775. (b) Crocker, L. S.; Heinekey, D. M. *J. Am. Chem. Soc.* **1989**, *111*, 405. (c) Cotton, F. A.; Wilkinson, G. *Advanced Inorganic Chemistry*, 5. edn; Wiley: Chichester; 1988.

$(PR_3)_2$.[23c] Unfortunately, the anionic species were too labile for obtaining reliable EPR spectra. The second one-electron reduction processes of **1a** and **2b** were found to be totally irreversible, presumably because of dissociative tendencies of the then d^8 configurated complexes (Table 1). The differences of about 1.85 V between the oxidation and reduction potentials of individual THF solvate complexes correlate well with the optical absorption maxima at about 550 nm (2.25 eV), the discrepancy of 0.4 (e)V being due to contributions from inter- and intramolecular relaxation.[24]

Dihydrogen Complex. Electrochemical studies of complexes suspected or known to contain dihydrogen ligands have been described for neutral and cationic systems.[25] When the oxidation of a solution of $(PCy_3)_2(CO)_3W$ in THF is not carried out under argon but under 1 atm H_2 pressure the yellow solution containing an equilibrium between dihydride and dihydrogen complex[2,3a] is oxidized irreversibly at a slightly lower potential than the THF solvate; a small cathodic peak appears which is shifted by about 0.36 V (Figure 2). Considering the variable but potentially high acidity of metal-coordinated dihydrogen[26] and in particular of oxidized polyhydride and dihydrogen complexes[25,27] we assume the loss of a proton to the basic solvent THF. Although the fate of the remaining metal hydride could not be further investigated (re-formation of the THF complex was not observed), a process such as (1) would be in agreement with data for other dihydrogen complexes[25a,b] and with the postulated mechanism of hydrogenase enzymes.[28,29]

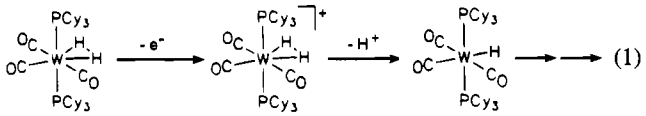

(1)

Electrochemical reduction of the dihydrogen/dihydride complex equilibrium was not observed within the accessible potential region which stands in agreement with the high-energy optical absorption (<400 nm) of this yellow solution in comparison to the THF solvate system.

Dinuclear Complexes: Stability and Electrochemistry. While the complexes **4a,b** and **5a,b** of pyrazine (pK_a 0.65)[30a,b] are less stable than corresponding mononuclear compounds with *N*-methylpyrazinium (pK_a about −5),[9,13,30a,b] the stronger basic but weaker π acidic bridging ligands bp (pK_a 4.82)[30c] and 4,4′-bptz[16] form the most labile complexes **6a** and **7a** with the $(PR_3)_2(CO)_3M$ fragments. Such a behavior is characteristic for back-donating organometal fragments, and accordingly, the "weak" ligand H_2 has been found to replace bound H_2O from $(P^iPr_3)_2(CO)_3W(H_2O)$ in *n*-hexane solution.[28] Unfortunately, the advantage of higher stability and better steric protection of the metal center by the PCy_3 ligands could not be used for the dinuclear systems because of the very poor solubility of these complexes.

Chart 3

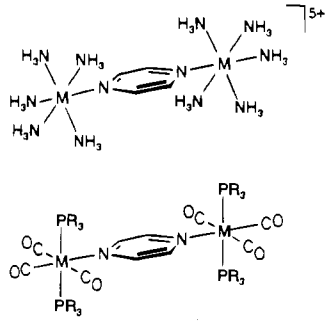

Cyclic voltammetry of the dinuclear P^iPr_3-containing complexes **4a**−**7a** revealed the expected[16,20,31] reduction of the bridging π-acceptor ligand in an apparently electrochemically reversible fashion. However, EPR results (Figure 9, Table 5) as discussed further below indicate that this reduction involves the loss of one phosphane ligand at each metal center. When compared to corresponding bis(pentacarbonylmetal) complexes,[32] the reduction potentials for the pz and bp systems are shifted to more negative values due to the replacement of two CO groups on each metal by more electron-rich trialkylphosphane ligands.[31] Nevertheless, the reduction is still facilitated in comparison to that of the free ligands, suggesting that the acceptor effect is not yet fully compensated by π-back-donation.[33] Coordination effects on the pyridyl-coordinated 4,4′-bptz ligand are negligible because the singly occupied MO (a_u) of 4,4′-bptz is localized at the four tetrazine nitrogen centers.[16]

For the symmetrically dinuclear pz and bp complexes the substitution of two axial CO groups by PR_3 ligands causes a small negative shift of the ligand-centered reduction but a large such shift for the metal-centered oxidation. In addition, the otherwise irreversible[32] $d^6 \rightarrow d^5$ oxidation process becomes reversible, allowing the stabilization and even isolation of some mixed-valent intermediates. In fact, the pyrazine-bridged complexes which bear a close resemblance to the Creutz-Taube system (Chart 3, M = Ru)[34] exhibit a rather large solvent-dependent splitting between two electrochemically reversible one-electron oxidation waves (Table 1). The comproportionation constants $K_c = 10^{(E_{ox2}-E_{ox1})/0.059V}$ are larger for the $5d^5/5d^6$ system $\mathbf{5a}^+$ than for the $4d^5/4d^6$ analogue $\mathbf{4a}^+$ under identical circumstances (Table 6). A rationalization for this relation in the case of π-acceptor bridged mixed-valent systems has been given earlier,[35] other examples include the ions $\{[(H_3N)_5M]_2(pz)\}^{5+}$, M = Ru, Os (Chart 3)[34,36] and bridged quadruply

(24) (a) Dodsworth, E.; Lever, A. B. P. *Chem. Phys. Lett.* **1985**, *119*, 61. (b) Dodsworth, E.; Lever, A. B. P. *Chem. Phys. Lett.* **1986**, *124*, 152. (c) Kober, E. M.; Goldsby, K. A.; Narayana, D. N. S.; Meyer, T. J. *J. Am. Chem. Soc.* **1983**, *105*, 4303.
(25) (a) Bianchini, C.; Laschi, F.; Peruzzini, M.; Ottaviani, F. M.; Vacca, A.; Zanello, P. *Inorg. Chem.* **1990**, *29*, 3394. (b) Zanello, P. *Comments Inorg. Chem.* **1991**, *11*, 339. (c) Costello, M. T.; Walton, R. A. *Inorg. Chem.* **1988**, *27*, 2563. (d) Harman, W. D.; Taube, H. *J. Am. Chem. Soc.* **1990**, *112*, 2261.
(26) (a) Chinn, M. S.; Heinekey, D. M.; Payne, N. G.; Sofield, C. D. *Organometallics* **1989**, *8*, 1824. (b) Schlaf, M.; Lough, A. J.; Morris, R. H. *Organometallics* **1993**, *12*, 3808.
(27) (a) Ryan, O. B.; Tilset, M.; Parker, V. D. *J. Am. Chem. Soc.* **1990**, *112*, 2618. (b) Ryan, O. B.; Tilset, M.; Parker, V. D. *Organometallics* **1991**, *10*, 298. (c) Zlota, A. A.; Tilset, M.; Caulton, K. G. *Inorg. Chem.* **1993**, *32*, 3816.
(28) Kubas, G. J.; Burns, C. J.; Khalsa, G. R. K.; Van der Sluys, L. S.; Kiss, G.; Hoff, C. D. *Organometallics* **1992**, *11*, 3390.
(29) (a) Crabtree, R. H. *Inorg. Chim. Acta* **1986**, *125*, L7. (b) Adams, M. W. W. *Biochim. Biophys. Acta* **1990**, *1020*, 115. (c) Kaim, W.; Schwederski, B. *Bioinorganic Chemistry*; Wiley: Chichester; 1994.
(30) (a) Chia, A. S.; Trimble, R. F. *J. Phys. Chem.* **1961**, *65*, 863. (b) Brignelli, P. J.; Johnson, C. D.; Katritzky, A. R.; Shakir, N.; Tarhan, H. O.; Walker, G. *J. Chem. Soc. B* **1967**, 2396. (c) Krumholz, P. *J. Am. Chem. Soc.* **1951**, *73*, 3487.
(31) Olbrich-Deussner, B.; Kaim, W. *J. Organomet. Chem.* **1989**, *361*, 335.
(32) (a) Pannell, K. H., Iglesias, R. *Inorg. Chim. Acta* **1979**, *33*, L161. (b) Lees, A. J.; Fobare, J.; Mattimore, E. *Inorg. Chem.* **1984**, *23*, 2709. (c) Zulu, M. M., Lees, A. J. *Inorg. Chem.* **1988**, *27*, 1139. (d) Gross, R.; Kaim, W. *Inorg. Chem.* **1986**, *25*, 498.
(33) Olbrich-Deussner, B.; Kaim, W.; Gross-Lannert, R. *Inorg. Chem.* **1989**, *28*, 3113.
(34) Creutz, C.; Taube, H. *J. Am. Chem. Soc.* **1969**, *91*, 3988. (b) Creutz, C.; Taube, H. *J. Am. Chem. Soc.* **1973**, *95*, 1086. (c) Creutz, C. *Prog. Inorg. Chem.* **1983**, *30*, 1.
(35) Kaim, W.; Kasack, V. *Inorg. Chem.* **1990**, *29*, 4696.
(36) Lay, P. A.; Magnuson, R. H.; Taube, H. *Inorg. Chem.* **1988**, *27*, 2364.

Table 6. Characteristic Data of Pyrazine-Bridged d^5/d^6 Mixed-Valent Dimers $[L_nM-(pz)-ML_n]^{m+}$

	L_nM				
	$W(CO)_3(P^iPr_3)_2$[a] ($m = 1$)	$Mo(CO)_3(P^iPr_3)_2$[a] ($m = 1$)	$Os(NH_3)_5$[b] ($m = 5$)	$Ru(NH_3)_5$[b] ($m = 5$)	$Fe(CN)_5$[b] $m = -5$
K_c	$10^{11.0}$	$10^{6.4}$ [c]	$10^{13.0}$	$10^{6.82}$	$10^{1.70}$
ν_{MLCT} (cm^{-1})	12720	12100	20330	17700	22200
ν_{MMCT} (cm^{-1})	4990	4650	11240	6400	8300
$\Delta\nu_{1/2}$ (cm^{-1})	730	700	1850	1250[d]	4800
ϵ (M^{-1} cm^{-1})	4600	7000	2700	5000	2200
g_1	2.197	2.0655		2.799[e]	
g_2	2.158	2.0655	n.r.	2.487	n.r.
g_3	1.931	1.9755		1.346	

[a] In CH_2Cl_2 (this work). [b] In H_2O or D_2O.[34,36,39] [c] In THF (Table 1). [d] Very unsymmetrical band. [e] From single crystal study.[46]

bonded dimers of molybdenum and tungsten.[37] The absolute values of K_c are similar for the Ru and Mo or Os and W systems, respectively (Table 6): however, the very different solvents have to be taken into account as evident from the effects listed in Table 1. Notably, the difference between 4d and 5d analogues is larger for the pentaamminemetal complexes (Chart 3) than for the carbonylmetal pair presented here (Table 6). The low oxidation potential, large K_c value, and relatively high persistence of **5a**$^+$ have allowed us to generate this species via oxidation with iodine and isolate it as the tetraphenylborate salt.

In contrast to the pyrazine-bridged system **5a**/**5a**$^+$/**5a**$^{2+}$ the bp- and (4,4′-bptz)-bridged analogues exhibit no discernible splitting of the two oxidation waves in the cyclic voltammograms (Figure 3). This result is in agreement with the K_c value estimated to be $10^{1.3}$ for $\{[(H_3N)_5Ru]_2(bp)\}^{5+}$;[34c] both the larger distance (through-space contribution)[38] and the smaller electronic coupling[35] via the poorer π-acidic bp and 4,4′-bptz ligands (through-bond effect) can be made responsible for this result.

Dinuclear Complexes: Spectroscopy and Spectroelectrochemistry. The stability of the monocationic and, to a lesser extent, the dicationic and monoanionic oxidation states has allowed us to measure and compare spectral data for several neighboring oxidation states of these complexes in order to gather as much information as possible on the electronic structures of the $(PR_3)_2(CO)_3M$ fragments and their effects on coordinated acceptor ligands. Since the studies of the Creutz–Taube ion and of related d^5/d^6 mixed-valent systems[34,36,39] have been enormously fruitful for the understanding of electron transfer and charge delocalization,[34] corresponding information on organometallic analogues should be highly valuable. Attempts to produce such species which can be expected to be less susceptible to charge trapping by the solvent have been unsuccessful in the past because dinuclear complexes of $M(CO)_5$ fragments, M = Cr, Mo, W, with μ-pyrazine (pz) are only irreversibly oxidized at high potentials.[32] Pyrazine-bridged dimers of the $(C_5R_5)(CO)_2Mn$ fragments, on the other hand, suffer from a pronounced dissociative lability[32d] and light-sensitivity which is caused by low-lying unoccupied d orbitals of the e_g set and which is accompanied by an unexpected paramagnetism of these 18 valence electron species.[40]

As recent work by Geiger et al. has demonstrated[17a,41] the use of carbonyl vibrational spectroelectrochemistry is very suitable to study questions concerning (de)localization in organometallic mixed-valent species, bearing in mind the rather short time-scale of about 10^{-12} s for infrared vibrational spectroscopy. Looking either at the two isolated molecules or at spectroelectrochemical results (Figures 4 and 7), the pyrazine-bridged complexes **4a** and **5a** show straightforward high-energy shifts of the three ν(CO) bands when going from the neutral via the cationic to the dicationic state (Figure 4).[12c] The mixed-valent forms in particular exhibit no unusual features in terms of two different metal carbonyl sites. According to the infrared data alone, the pyrazine-bridged monocations have thus to be formulated as fully delocalized species $\{[(P^iPr_3)_2(CO)_3M^{0.5}]_2(\mu\text{-pz})\}^+$. A similar conclusion was reached for the Creutz–Taube ion using less defined vibrations;[42] more localized situations have been found with π-coordinating ligand bridges as described by Geiger et al.[17a,41] Following up to the second oxidation of **5a** it appears that the central band (b_{2u}) experiences the largest high-energy shift because of the most pronounced reduction of W → CO π back-donation for this asymmetric vibration mode (Table 3).

In their neutral states the pyrazine-bridged dinuclear complexes exhibit unique absorption spectra with one intense and extraordinarily narrow band in the near infrared region (Figure 5, Table 4). This band is readily attributed to the allowed metal-to-ligand charge transfer (MLCT) transition $d_{xz} \rightarrow \pi^*$, it is accompanied by a high energy shoulder, tentatively ascribed to d_{yz}, $d_{xy} \rightarrow \pi^*$ components.[32b,c] Shape, bandwidth, and absorption maxima of the main CT band are solvent-dependent, the slight negative solvatochromism observed can be correlated with established solvent parameters E_{MLCT}:[18] $\nu = 16000\ cm^{-1} + 1485\ cm^{-1} \times E_{MLCT}$ (**5a**). The MLCT absorption band is narrowest in nonpolar solvents, indicating an unusually small amount of inter- and intramolecular geometrical reorganization between ground and MLCT excited state. This result is all the more surprising as the $M(CO)_5$ analogues show much broader bands in the visible region with typical CT bandwidths of 4000 cm^{-1};[12a,32] the complexes **4a**–**7a**, on the other hand, with four conformationally flexible P^iPr_3 groups and thus very many structural degrees of freedom exhibit some of the narrowest metal-to-ligand charge transfer bands yet observed in solution at ambient temperatures. The small reorganization energy is also evident when the rather low energies E_{op} of the MLCT (HOMO → LUMO) transitions (in eV) are compared with the differences $\Delta E = E_{ox1} - E_{red1}$ (in V). For the best studied

(37) Cayton, R. H.; Chisholm, M. H.; Huffman, J. C.; Lobkovsky, E. B. *J. Am. Chem. Soc.* **1991**, *113*, 8709.
(38) (a) Allen, G. C.; Hush, N. S. *Prog. Inorg. Chem.* **1967**, *8*, 357. (b) Hush, N. S. *Prog. Inorg. Chem.* **1967**, *8*, 391.
(39) (a) Felix, F.; Hauser, U.; Siegenthaler, H.; Wenk, F. *Inorg. Chim. Acta* **1975**, *15*, L7. (b) Felix, F.; Ludi, A. *Inorg. Chem.* **1978**, *17*, 1782.
(40) Kaim, W.; Roth, T.; Olbrich-Deussner, B.; Gross-Lannert, R.; Jordanov, J.; Roth, E. K. H. *J. Am. Chem. Soc.* **1992**, *114*, 5693.
(41) (a) Van Order Jr., N.; Bitterwolf, T. E.; Rheingold, A. L.; Geiger, W. E. *J. Am. Chem. Soc.* **1987**, *109*, 5680. (b) Geiger, W. E.; Van Order Jr., N.; Pierce, D. T.; Bitterwolf, T. E.; Rheingold, A. L.; Chasteen, N. D. *Organometallics* **1991**, *10*, 2403. (c) Geiger, W. E.; Atwood, C. G.; Chin, T. T. in *Molecular Electrochemistry of Inorganic, Bioinorganic and Organometallic Compounds* (Pombeiro, A. J. L.; McCleverty, J. A., eds.); Kluwer Academic Publishers: Dordrecht; 1993, p 519. (d) Merkert, J. W.; Geiger, W. E.; Paddon-Row, M. N.; Oliver, A. M.; Rheingold, A. L. *Organometallics* **1992**, *11*, 4109. (e) Pierce, D. T.; Geiger, W. E. *Inorg. Chem.* **1994**, *33*, 373.
(42) Best, S. P.; Clark, R. J. H.; McQueen, C. S.; Joss, S. *J. Am. Chem. Soc.* **1989**, *111*, 548.

example **5a** in CH_2Cl_2, this difference[24] $\chi = E_{op} - \Delta E = 1.38$ eV − 1.34 V is much smaller than the values calculated for ruthenium polypyridine complexes,[24] let alone other metal carbonyl systems.[16,18,31-33]

At least three ligand-field transitions (d → d), otherwise often obscured by broad charge transfer features in the visible,[32b,c] appear as well detectable bands in the spectra of the neutral dinuclear complexes; their relatively high intensity ($\epsilon \approx 1000$ M^{-1} cm^{-1}) is similar to that of other metal carbonyl systems.[32b-c] Intraligand (IL) transitions occur only in the UV region, beyond 33000 cm^{-1} (Figure 5).

The bp and 4,4′-bptz bridged complexes **6a** and **7a** show similar spectra as the compounds bridged by pz, however, their tendency to dissociate did not permit a reliable determination of solvatochromic effects or LF absorptions. The comparison between optical and electrochemical data reveals a slightly higher amount of reorganization energy χ in relation to the pz-bridged analogues. The lower MLCT energy of **4a** as compared to the 5d analogue **5a** results from a stabilization of d orbitals in the latter complex.

On oxidation, the MLCT band becomes broader, weaker and hypsochromically shifted due to a stabilization of d orbitals, similar observations were made for the $\{[(H_3N)_5Os]_2(pz)\}^{n+}$ system.[36] The CT band now shows weak positive solvatochromism, i.e. a small bathochromic shift in more polar solvents. The LF transitions are also hypsochromically shifted; however, the most salient new feature is the appearance of a very long-wavelength absorption band, attributable to an intervalence transfer (IT) or metal-to-metal charge transfer (MMCT) transition in a localized picture;[43] for a delocalized system, such transitions should rather be described as a transition from a bonding combination of d_{xz} orbitals to a weakly antibonding combination.[34c,36] These bands are quite intense and much more symmetrical than the corresponding feature of the Creutz−Taube ion.[34] The Mo analogue shows an additional bathochromic shift relative to the tungsten system which is not unexpected considering the d → d nature of this transition and the precedent from the ions $\{[(H_3N)_5M]_2(pz)\}^{5+}$, M = Ru, Os (Table 6). Also in agreement with the inorganic systems of Chart 3 is the higher intensity of the band for the 4d analogue (Table 6). The virtually absent solvatochromism points to a class III system according to the classification by Robin and Day,[43a] i.e. to a fully delocalized system. Table 6 compares electrochemical, optical and EPR features of the Creutz−Taube ion and related systems with those of the organometallic analogues described here. Both the Hush formula (although not applicable for delocalized systems)[34c,38,44] and the 50% value of the absorption energy as an approximate measure of the interaction energy[44] suggest that this energy is smaller for the carbonylmetal species than for the Creutz−Taube ion or its Os(III/II) analogue.

Unfortunately, the class III character of the mixed-valent systems which is evident from vibrational and electronic absorption spectroscopy could not be positively supported by EPR for the tungsten complexes because of high line width and apparently small metal isotope and ^{31}P coupling constants. However, the solution spectrum of the dimolybdenum complex $\mathbf{4a}^+$ yielded such information in the form of $^{95,97}Mo$ isotope coupling with the appropriate satellite splitting pattern for two equivalent metal nuclei and a coupling constant about half as large as that of the corresponding mononuclear Mo(I) complex $[(P^iPr_3)_2(CO)_3Mo(pz)]^+$.[12d] These metal isotope coupling constants (Table 2) are distinctly smaller by about 50% in comparison to those of other Mo(I) (≈5 mT) or delocalized Mo(I)/Mo(0) systems (≈2.5 mT)[45a] which, in the absence of detectable ^{31}P coupling (<0.4 mT for $\mathbf{4a}^+$), suggests significant M/CO covalency and the occupation of the d_{xy} orbital by the single electron; the $(d_{xz})^2(d_{yz})^2(d_{xy})^1$ configuration is fully compatible with a six-coordinate d^5 metal and predominantly axial distortion. The covalency is also evident from the powder EPR data of the mixed-valent cations which show a similar pattern $g_1 > g_2 > g(\text{electron}) > g_3$ as the Creutz−Taube system[45b] (Table 6), albeit with a much less pronounced g spread, $g_1 - g_3$. Due to the higher spin-orbit coupling factor the difference $g_1 - g_3$ is larger for the tungsten system $\mathbf{5a}^+$ than for the Mo analogue $\mathbf{4a}^+$. In comparison to the THF complexes $\mathbf{1a}^+$ and $\mathbf{2a}^+$, the dinuclear pyrazine-bridged cations show slightly lower g components but a similar anisotropy $g_1 - g_3$ which clearly points to metal-centered paramagnetism in contrast to that of related stable *N,N′*-dialkyl-substituted radical cations (Chart 4).[46]

Chart 4

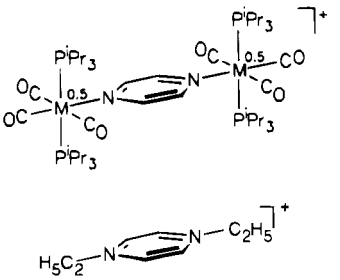

Reduction of the dinuclear complexes with pz or bp as bridging ligands yields the expected[19,20] anion radical complexes $M^0-(\mu\text{-}L^{-\bullet})-M^0$; W(−I) species, on the other hand, would have very different EPR characteristics.[47] In combination with the metal-centered processes of oxidation this acceptor ligand-centered reduction thus supports the MLCT nature of the lowest-lying excited states. At first glance, the coupling constants of ^{14}N, ^{1}H, $^{95,97}Mo$ and ^{183}W nuclei and the g factors of $\mathbf{4a}^{-\bullet}$, $\mathbf{5a}^{-\bullet}$, and $\mathbf{6a}^{-\bullet}$ are very similar to those of related symmetrically dinuclear pentacarbonylmetal or tetracarbonylmetal complexes (Table 5).[20] However, the ^{31}P coupling constants reveal an initially surprising result: Only one coupling P nucleus is observed for each tricarbonylmetal center with hyperfine splittings more than twice as large as those observed for P-ligand containing tetracarbonylmetal derivatives (Table 5). Coupling from the "missing" ^{31}P nuclei is not detected within the limits of the very small line widths of less than 0.05 mT (Figure 9). Obviously, a dissociation of one of the two PR_3 ligands per metal center occurs on electron uptake despite an apparently electrochemically reversible reduction (Figure 3). Due to lack of spectroscopic information the number of PR_3 ligands could not be established for the reduced (4,4′-bptz)-bridged system $\mathbf{7a}^{-\bullet}$, however, a similar dissociation had already been observed for the mononuclear *N*-methylpyrazinium complexes $[(mpz)M(CO)_3(PR_3)_2]^+$.[9]

For an explanation of this effect one has to remember that the $(PR_3)_2(CO)_3M$ fragments are quite electron-rich and that the additional amount, $\delta-$, of negative charge transmitted from the reduced and thus π-basic rather than π-acidic bridging anion

(43) (a) Robin, M. B.; Day, P. *Adv. Inorg. Chem. Radiochem.* **1967**, *10*, 247. (b) Blasse, G. *Struct. Bonding (Berlin)* **1991**, *76*, 153.
(44) Richardson, D. E.; Taube, H. *J. Am. Chem. Soc.* **1983**, *105*, 40.
(45) (a) Das, A.; Jeffery, J. C.; Maher, J. P.; McCleverty, J. A.; Schatz, E.; Ward, M. D.; Wollermann, G. *Inorg. Chem.* **1993**, *32*, 2145. (b) Stebler, A.; Ammeter, J. H.; Fürholz, U.; Ludi, A. *Inorg. Chem.* **1984**, *23*, 2764.
(46) Kaim, W.; Schulz, A.; Hilgers, F.; Hausen, H.-D.; Moscherosch, M.; Lichtblau, A.; Jordanov, J.; Roth, E.; Zalis, S. *Res. Chem. Intermed.* **1993**, *19*, 603.
(47) Hynes, R. C.; Preston, K. F.; Springs, J. J.; Williams, A. J. *J. Chem. Soc. Dalton Trans.* **1990**, 3655.

radical ligands can cause dissociation of one of the most labile ligands, i.e. one of the bulky trialkylphosphines. The coordination site left by that PR_3 ligand could either be occupied by a THF solvent molecule or remain free; the distinctly increased ^{31}P coupling constants suggest a significant deviation from octahedral symmetry and thus a pentacoordinate situation as was assumed for the 17 valence electron d^7 species $[(PR_3)_2(CO)_3M]^-$. The metal center would thus adopt a $16 + \delta$ rather than an $18 + \delta$ valence electron structure[31,48] because the latter would involve *three* electron-rich ligands, i.e. two trialkylphosphane molecules ($pK_a > 7.5$) and an anion radical. In fact, pentacoordinate tricarbonylmanganese[49a] and -tungsten complexes[49b] with σ and π donating catecholate ligands were structurally characterized as stable 16 valence electron species. The very negative reduction potentials of the dinuclear complexes discussed here have so far precluded spectroelectrochemical investigations, however, further attempts will be made in that direction.

Conclusions

The dinuclear complexes of the $(PR_3)_2(CO)_3M$ fragments with the conjugated bridging ligands (Chart 2) are distinguished by very narrow charge transfer absorption features and thus unusually small MLCT reorganization effects of the M^0/M^0 forms, by stable and delocalized M^I/M^0 oxidation states in the case of the pyrazine-bridged systems, and by the loss of PR_3 on reduction to the M^0/M^0 anion radical complexes. These effects point to a very special combination of properties of the $M(CO)_3(PR_3)_2$ complex fragment, including the ability to sterically protect a small ligand and an electronic situation favoring a carefully balanced electron donation/acceptance interaction as required for binding of H_2 (Chart 1).

The characteristics of H_2 as a σ-donor/σ^*-acceptor ligand may be tentatively quantified via the metal-centered oxidation which is facilitated by σ-donor contributions and made more difficult by σ^* or π^* acceptor effects. Taking the oxidation potential as one such measure[50] for the combined donor/acceptor effect and assuming a small difference $E_{1/2} - E_{pa}$, one arrives at a sequence $mpz^+ > pz > H_2 > 4,4'$-bptz > bp > THF (Table 7) which would place H_2 right between the good (mpz^+, pz) and the poor π acids (bp, 4,4′-bptz, THF) described here.

Therefore, it is not surprising that the $[M(NH_3)_5]^{2+}$ fragments (M = Ru,Os) which exhibit strong π type interactions with pyrazine[36] are also well suited to coordinate and activate H_2.[25d]

Table 7. W(0)/W(I) Oxidation Potentials[a]

complex (W(0) form)	E_{ox}	electrolyte
$(mpz^+)W(CO)_3(PCy_3)_2$[b]	+0.13	THF/0.1 M Bu_4NPF_6
$(mpz^+)W(CO)_3(P^iPr_3)_2$[b]	+0.08	THF/0.1 M Bu_4NPF_6
$(pz)[W(CO)_3(P^iPr_3)_2]_2$	−0.01/−0.51[c]	THF/0.1 M Bu_4NClO_4
$(pz)[W(CO)_3(P^iPr_3)_2]_2$	−0.01/−0.71[c]	THF/0.05 M Bu_4NBPh_4
$(H_2)W(CO)_3(PCy_3)_2$	−0.40[d]	THF/0.05 M Bu_4NBPh_4
$(4,4'$-bptz$)[W(CO)_3(P^iPr_3)_2]_2$	−0.43	THF/0.05 M Bu_4NBPh_4
$(bp)[W(CO)_3(P^iPr_3)_2]_2$	−0.48	THF/0.05 M Bu_4NBPh_4
$(THF)W(CO)_3(PR_3)_2$[e]	−0.69	THF/0.05 M Bu_4NBPh_4

[a] Potentials in V vs. Fc/Fc^+. [b] From ref 9. [c] Split waves for two one-electron processes. [d] Peak potential at 200 mV/s for irreversible wave. [e] R = ^{i}Pr or Cy.

Acknowledgment. This work has been supported by Deutsche Forschungsgemeinschaft (SFB 270), by an exchange program between the DFG and the Czech Academy of Sciences and by the Fonds der Chemischen Industrie.

IC940857V

(48) (a) Olbrich-Deussner, B.; Kaim, W. *J. Organomet. Chem.* **1988**, *340*, 71. (b) Kaim, W.; Olbrich-Deussner, B.; Gross, R.; Ernst, S.; Kohlmann, S.; Bessenbacher, C. in *Importance of Paramagnetic Organometallic Species in Activation, Selectivity and Catalysis* (Chanon, M., ed.); Kluwer Academic Publishers: Dordrecht; 1989, p 283. (c) Mao, F.; Tyler, D. R.; Bruce, M. R. M.; Bruce, A. E.; Rieger, A. L.; Rieger, P. H. *J. Am. Chem. Soc.* **1992**, *114*, 6418.

(49) (a) Hartl, F.; Vlcek Jr., A.; deLearie, L. A.; Pierpont, C. G. *Inorg. Chem.* **1990**, *29*, 1073. (b) Darensbourg, D. J.; Klausmeyer, K. K.; Mueller, B. L.; Reibenspies, J. H. *Angew. Chem. Int. Ed. Engl.* **1992**, *31*, 1503.

(50) (a) Pickett, C. J.; Pletcher, D. *J. Organomet. Chem.* **1975**, *102*, 327. (b) Chatt, J.; Kan, C. T.; Leigh, G. J.; Pickett, C. J.; Stanley, D. R. *J. Chem. Soc., Dalton Trans.* **1980**, 2032.